Physicochemical Characterization and Antioxidant Activity of Quercetin-Loaded Chitosan Nanoparticles

Yuying Zhang, Yan Yang, Kai Tang, Xing Hu, Guolin Zou

State Key Laboratory of Virology, College of Life Sciences, Wuhan University, 430072 Wuhan, People's Republic of China

ABSTRACT: Quercetin is an abundant flavonoid in food plants with numerous biological activities and widely used as a potent antioxidant. Being sparingly soluble in water and subject to degradation in aqueous intestinal fluids, the absorption of quercetin is limited upon oral administration. In the present study, chitosan nanoparticles and quercetin-loaded nanoparticles were prepared based on the ionic gelation of chitosan with tripolyphosphate anions. The encapsulation of quercetin in the chitosan nanoparticles were confirmed by differential scanning calorimetry, X-ray powder diffractometry, Fourier transformed infrared spectroscopy, ultraviolet-visible spectrum, and fluorescence spectrum. The morphology of the nanoparticles was characterized by atomic force microscopy. The antioxidant activity of the quercetin-nanoparticles was also evaluated *in vitro* by two different methods (free radical scavenging activity test and reducing power test), which indicates that inclusion of quercetin in chitosan nanopaticles may be useful in improving the bioavailabilty of quercetin. © 2007 Wiley Periodicals, Inc. J Appl Polym Sci 107: 891–897, 2008

Key words: quercetin; chitosan; nanoparticles; characterization; antioxidant

INTRODUCTION

In recent years, flavonoids have attracted a great interest as potential therapeutic agents against a large variety of diseases, most of which involve radical damage.[1,2] Quercetin [Fig. 1(A)], 3,3',4',5'-7-pentahydroxy flavone, is one of the most abundant flavonoids in the human diet.[3] It has been demonstrated to possess a myriad of biological activities that are considered beneficial to health, including antioxidative, free radical scavenging, anticancer, and antiviral activities.[4–6] In spite of this wide spectrum of pharmacological properties, the use of quercetin in pharmaceutical field is limited by its low aqueous solubility.[7] In addition, it is chemically unstable, especially in aqueous alkaline medium, which possibly involves the attack of hydroxyl ions on the C-ring of quercetin.[8]

While in pharmaceutical product development, polymer nanoparticles have been widely investigated as a carrier for drug delivery.[9,10] Chitosan, the second abundant polysaccharide and a cationic polyelectrolyte present in nature,[11] is the deacetylated form of chitin and composed of glucosamine, known as (1-4)-2-amino-2-deoxy-β-D-glucose [Fig. 1(B)]. Properties such as biodegradability, low toxicity, and good biocompatibility make it suitable for use in biomedical and pharmaceutical formulations.[12–15] Particularly, Chitosan has been used in improving the dissolution rate of the poorly soluble drugs,[16] preparation of mucoadhesive formulations,[17–19] drug targeting,[20] and enhancement of peptide absorption.[21] Tripolyphosphate (TPP) [Fig. 1(C)] is a polyanion, which can interact with the cationic chitosan by electrostatic forces.[22,23] The method of complexation between oppositely charged molecules to prepare chitosan microspheres has attracted much attention because the process is very simple and mild.[11,24] The bioadhesive polysaccharide chitosan nanoparticles are used to provide controlled release of drugs and to improve the bioavailability of degradable substances.

The present study was designed to investigate the feasibility of encapsulating quercetin into chitosan nanoparticles to enhance its applications in pharmaceutical field. The nanoparticles were prepared by the method of ionic gelation and the structural characteristics of the inclusion complexes have been examined by differential scanning calorimetry, X-ray powder diffractometry, absorption spectrum, and fluorescence spectrum. The antioxidant activity of the quercetin-loaded nanoparticles was afterwards evaluated.

Correspondence to: G. Zou (zouguolin@whu.edu.cn).

WILEY
InterScience®
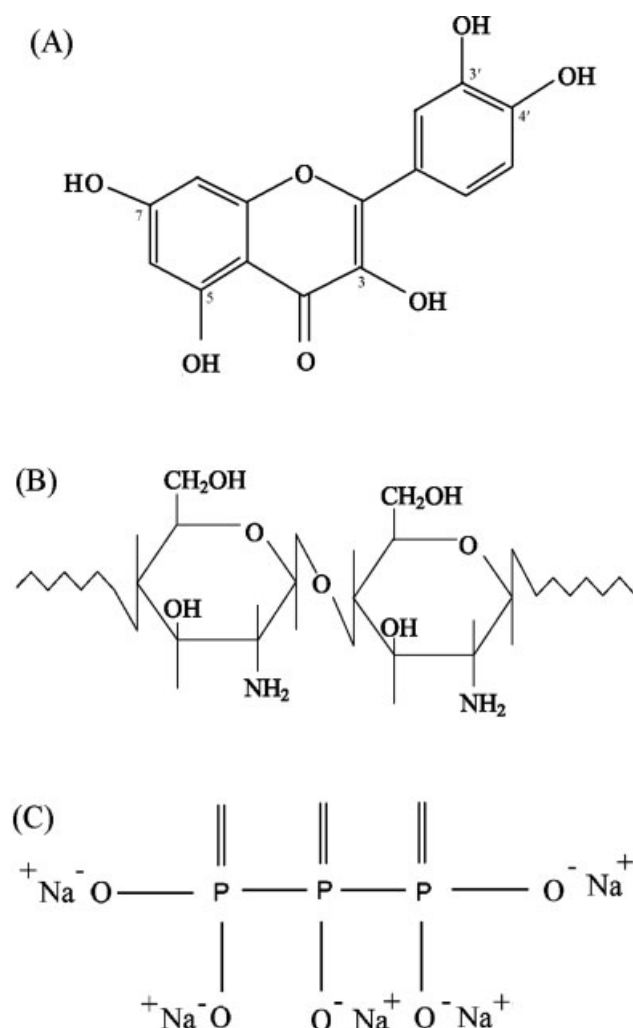DISCOVER SOMETHING GREAT

Figure 1 Chemical structure of quercetin (A), chitosan (B), and sodium tripolyphosphate (C).

EXPERIMENTAL

Materials

Quercetin, chitosan, TPP, and 1,1-diphenyl-2-picryl-hydrazyl radical (DPPH) were purchased from sigma (St. Louis, MO). The deacetylation degree of chitosan was 79% and the average molecular weight was 500,000, which obtained by using an Ubblelohde capillary viscometer at $(25 \pm 0.1)°C$. All other reagents used were of analytical regent grade. Solutions were prepared using water filtered through a MILLI-Q water system (Miliipore, Bedford, MA).

Methods

Preparation of chitosan nanoparticles and quercetin-loaded nanoparticles

Chitosan nanoparticles were prepared according to the literature based on the ionic gelation of chitosan with TPP anions.[25,26] Chitosan was dissolved in

acetic aqueous solution at 2 mg/mL and the concentration of acetic acid in aqueous solution was 3 vol %. Under magnetic stirring at room temperature, 4 mL TPP aqueous solution with concentration of 2 mg/mL was added into 10 mL chitosan solution. Opalescent suspension was formed spontaneously. The hydrodynamic diameter and zeta potential of nanoparticles were measured by a dynamic light scattering Zetasizer (Malvern 3000HSa, UK) to be 40–100 nm and +30.3 mV, respectively.

Quercetin-loaded nanoparticles were formed upon incorporation of 4 mL TPP solution containing quercetin into 10 mL chitosan solutions. The nanopaticles were separated from the aqueous medium containing nonassociated quercetin by ultracentrifugation at 40,000g, 4°C for 30 min and lyophilized.

Atomic force microscopy

A scanning probe Microscope SPM-9500 J3 instrument (Shimadzu, Japan) was used for visualization of both the chitosan nanoparticles and the quercetin-loaded chitosan nanoparticles deposited on glass substrate. The measurement was performed in tapping mode using a silica carbide probe under normal atmospheric conditions, at a temperature of 25°C.

Differential scanning calorimetry

Calorimetric measurements were carried out on a Netzsch-DSC200 PC Differential scanning calorimeter (Germany) at a heating rate of 10°C/min. Samples (1.8 mg) were accurately weighed using a Sartorius BS 110S electronic microbalance and heated in closed aluminum crimped cells over the temperature range of 30–360°C under a nitrogen flow of 40 mL/min.

X-ray powder diffractometry

Powder X-ray diffraction patterns (XRPD) were taken with a Bruker D8-Advance X-ray diffractometer (Germany), by using a Ni-filtered Cu Kα radiation over the 2θ range of 2–50°. Samples were finely ground in glass substrate and the experimental parameters were set as: voltage, 40 kV; current, 20 mA; angular speed, 4°/min. The XRPD patterns of quercetin, chitosan as well as the quercetin-loaded chitosan nanoparticles were recorded.

Spectroscopy characterization

The Fourier transform infrared (FTIR) spectra of quercetin, chitosan nanoparticles, and quercetin-loaded nanoparticles were recorded on a Nicolet 5700 FTIR spectroscopy (Thermo, USA) using a Smart OMNI-sampler Accessory. The scanning range was 400–4000 cm^{-1} and the resolution was 1 cm^{-1}.

An Australian Varian Cary-5000 spectrophotometer with a diffuse reflection integral sphere accessory was used for obtaining the ultraviolet-visible (UV-Vis) spectra. The scanning range was 190–800 nm and data interval was 1.0 nm.

Intrinsic fluorescence emission spectra between 350 nm and 650 nm were recorded with an F-4500 fluorescence spectrophotometer (Hitachi, Japan) equipped with a xenon lamp source using a 3-D scanning mode. Excitation and emission bandwidths were both set at 2.5 nm.

Measurement of free radical scavenging activity

The free radical scavenging activity of chitosan nanoparticles and quercetin-loaded nanoparticles was measured by DPPH according to literature with minor modifications.[27] Briefly, varying concentrations of chitosan nanoparticles or quercetin-loaded nanoparticles were added into 500 μL of DPPH solution (0.2 mM, in 50% ethanol). The reaction mixture was incubated in a shaker at room temperature for 30 min and the absorbance at 517 nm was read against a blank. Decreased absorbance of DPPH indicates increased antioxidant effect. The radical scavenging activity was calculated using the following equation:

Scavenging effect (%)
$$= (1 - A_{\text{samples, 517 nm}}/A_{\text{control, 517 nm}})$$
$$\times 100$$

Measurement of reducing power

The reducing power of chitosan nanoparticles and quercetin-loaded nanoparticles was quantified according to the method described earlier by Yen and Chen with minor modifications.[28] Briefly, 2 mL of reaction mixture, containing different concentration of nanoparticles in phosphate buffer (0.2M, pH 6.6), was incubated with 1 mL potassium ferricyanide (1% w/v) at 50°C for 20 min. By adding 1 mL trichloroacetic acid solution (10%, w/v) the reaction was terminated and the mixture was centrifuged at 5000 rpm for 5 min. The supernatant was mixed with distilled water and ferric chloride (0.1%, w/v) solution. The absorbance of the reaction mixture was measured at 700 nm and increased absorbance indicated increased reducing power.

RESULTS AND DISCUSSION

Atomic force microscopy

Atomic force microscopy (AFM) measurement is an effective method to provide the surface morphology.[29] As presented in Figure 2, 2 μm × 2 μm scans were captured. Image (a) is the morphology of chitosan nanoparticles and image (b) is of quercetin-loaded nanoparticles. It appears that the nanospheres were uniform and ellipsoidal in shape with smooth surfaces in both the two images. However, the size of the blank chitosan nanoparticles is smaller compared to the quercetin-loaded nanoparticles. Combining AFM image with SPM-9500 analysis, we may get an insight into the average particle size, which is about 68.08 nm for the blank and 76.58 nm for the quercetin-loaded chitosan nanoparticles, respectively. The results indicated that the loading of quercetin leads to an increase of the particle size.

Differential scanning calorimetry

Differential scanning calorimetry (DSC) was employed to check any variation of crystalline properties of
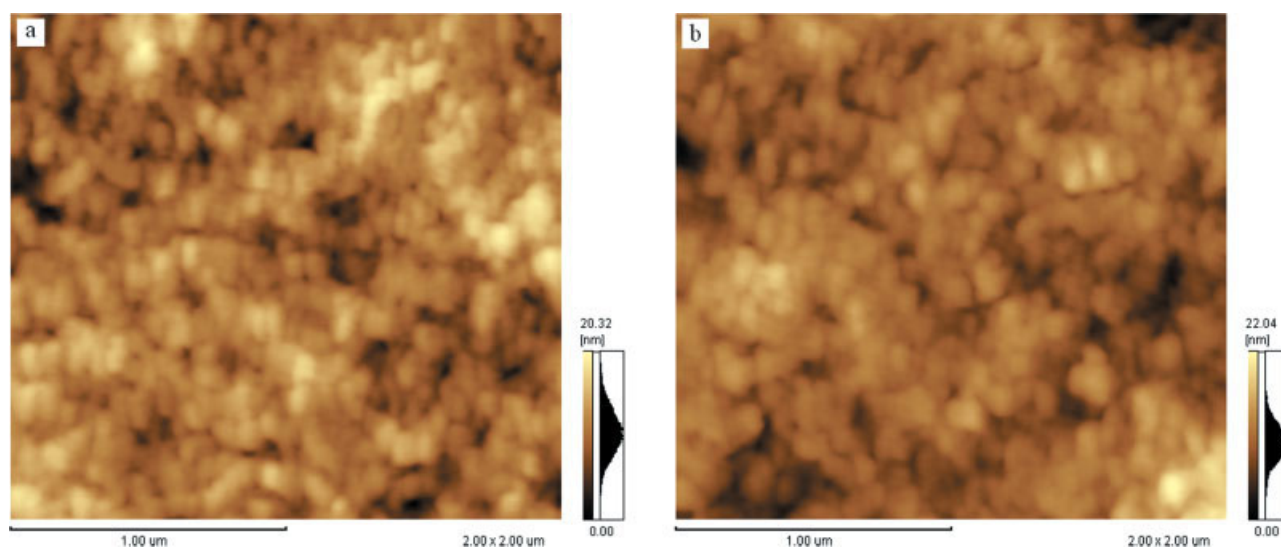

Figure 2 Atomic force micrographs of chitosan nanoparticles (a) and quercetin-loaded nanoparticles (b). [Color figure can be viewed in the online issue, which is available at www.interscience.wiley.com.]
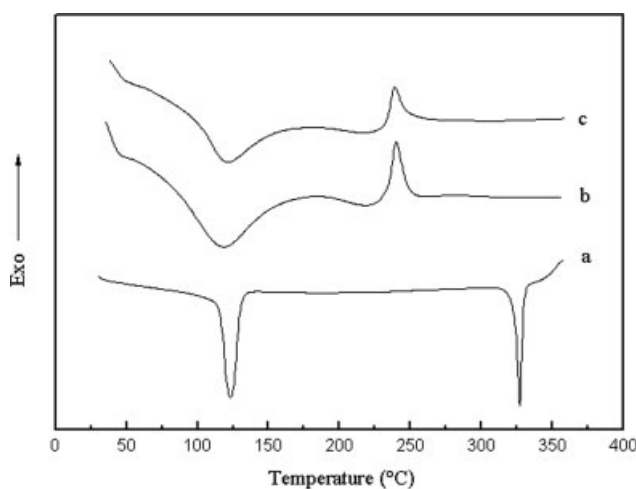
Figure 3 DSC curves of quercetin (a), chitosan nanoparticles (b), and quercetin-loaded nanoparticles (c).

quercetin because of the encapsulation into the chitosan nanoparticles.[1] The thermal curves of quercetin, chitosan nanoparticles, and quercetin-loaded nanoparticles are presented in Figure 3. It can be seen in the DSC curve quercetin showed a broad endothermic peak (T_{onset} = 116.0°C, T_{peak} = 123.3°C) as it becomes anhydrous and a melting endotherm (T_{onset} = 324.1°C; T_{peak} = 327.2°C). Broader endotherm was associated with loss of bound water from chitosan nanoparticles (T_{onset} = 82.1°C; T_{peak} = 118.6°C) and quercetin-loaded nanoparticles (T_{onset} = 98.3°C; T_{peak} = 121.5°C) while the characteristic, well recognizable thermal profile of quercetin corresponding to its melting point disappeared, which can be assumed as proof of inclusion of quercetin into the chitosan nanoparticles.
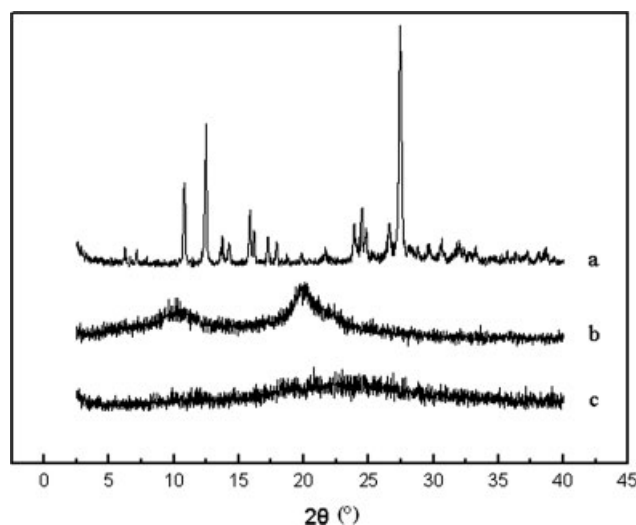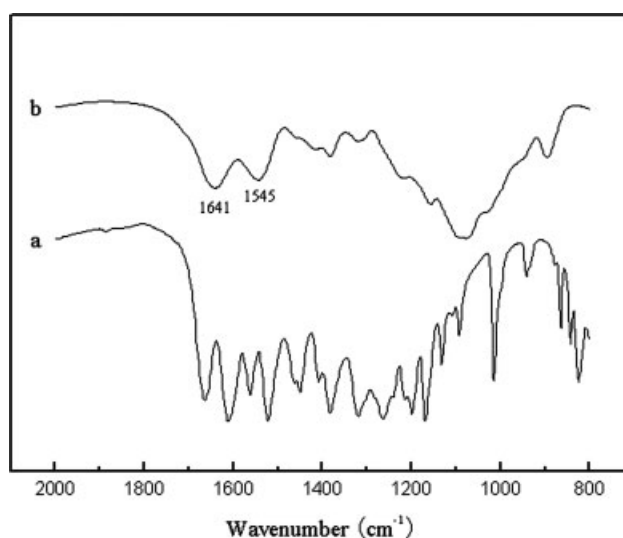

Figure 5 FTIR spectra of quercetin (a) and quercetin-loaded nanoparticles (b).

XRPD

Figure 4 shows the XRPD of quercetin, chitosan raw material, and quercetin-loaded nanoparticles. In the X-ray diffractogram of quercetin powder, sharp peaks at a diffraction angle of 2θ = 10.78°, 12.48°, 15.88°, 23.92°, 24.50°, 27.46° are present which suggest that the drug is present as a crystalline material.[7] There are also two strong peaks in the diffractogram of chitosan at 2θ = 10.30°, 20.12°, indicating the crystallinity of chitosan. However, the diffraction peaks relevant to crystalline quercetin and chitosan were no longer detectable in the quercetin-loaded nanoparticles, thus meaning a greater amorphousness of the inclusion compounds, compared to the free molecules. These results, confirmed that quercetin is no longer present as a crystalline material after
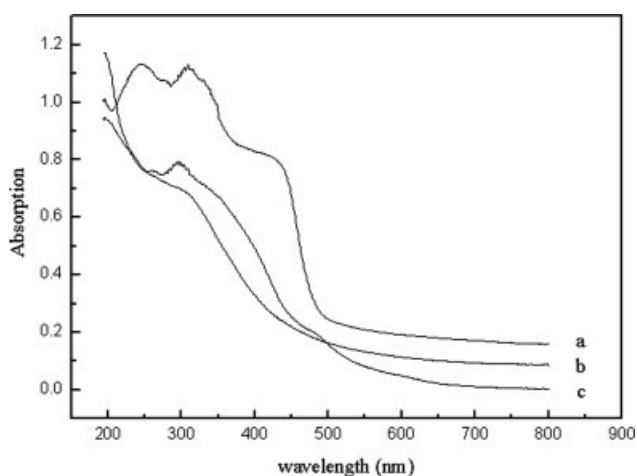

Figure 4 XPRD spectra of quercetin (a), chitosan (b), and quercetin-loaded nanoparticles (c).

Figure 6 UV-Vis spectra of quercetin (a), chitosan nanopaticles (b), and quercetin-loaded nanoparticles (c).
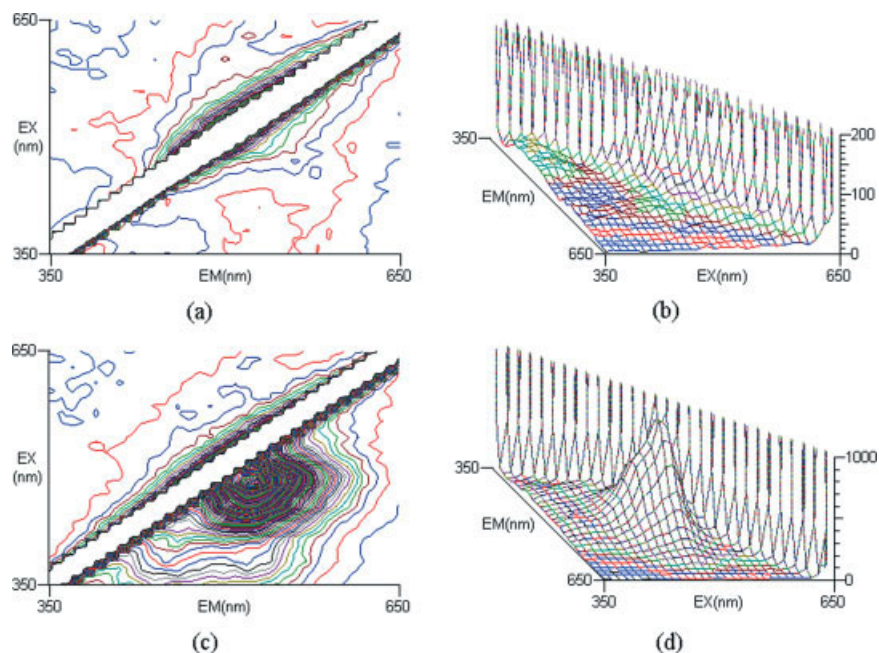
Figure 7 Fluorescence spectrum of (a) contour and (b) 3-D view of quercetin; (c) contour and (d) 3-D view of quercetin-loaded nanoparticles.

encapsulation and quercetin-loaded nanoparticles exist in the amorphous state.

Spectroscopy properties

Diffuse reflectance is a very effective technique in the analysis of powders, or whenever the roughness of the analyte surface is not negligible for the incident radiation wavelength.[1] During this experiment, a Smart OMNI-sampler Accessory was adopted to detect the absorption features on the surfaces of the powder. As shown in Figure 5, for the FTIR spectra of the quercetin-loaded nanoparticles, the characteristic bands of free quercetin, associated with aromatic bending and stretching (around 1100 and 1600 cm^{-1}), —OH phenolic bending (1200–1400 cm^{-1}) disappeared, while the absorption peaks assigned to C=O (1641 cm^{-1}), —NH bending vibration (1545 cm^{-1}) in amide group, and —C—O—C (1040–1150 cm^{-1}) in glycosidic linkage of chitosan appeared. It can be concluded that quercetin was not present on the surface but included in the nanoparticles.

The UV-Vis spectra of free quercetin, chitosan, and quercetin-loaded nanoparticles are presented in Figure 6. The spectrum of quercetin is quite different after inclusion in chitosan nanoparticles. Free quercetin powder showed an absorption band at 430 nm, of which the intensity decreased significantly and the position exhibited appreciable Einstein shift in the spectra of quercetin-loaded nanoparticles. The characteristic band of free powder at 245 nm disappeared and another band at 309 nm moved to 297 nm after encapsulation by chitosan. This result

definitely proves an interaction between quercetin and chitosan, since in the case of a physical mixture only a superimposition of the signals would have been observed.

Quercetin is weakly fluorescent and extremely sensitive to the surrounding medium such as polarity and hydrogen bonding effects.[30] Figure 7 shows the contour and 3-D view of quercetin powder and quercetin-loaded nanoparticles. It can be seen the encapsulation of quercetin into the chitosan nanoparticles causes a dramatic enhancement in the fluorescence emission intensity ($\lambda_{Exitation, max} = 481$ nm, $\lambda_{Emission, max} = 530$ nm), which indicates the variation of microenvironment. This is most because
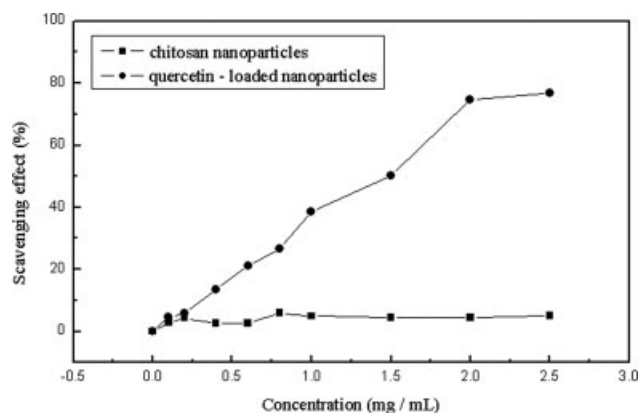

Figure 8 Scavenging effect of chitosan nanoparticles and quercetin-loaded nanoparticles on 1,1-diphenyl-2-picryl-hydrazyl radical. Each value is expressed as mean ± SD ($n = 3$).
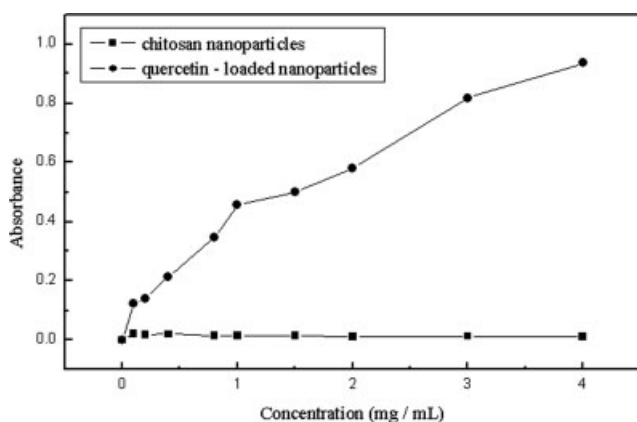
Figure 9 Reducing power of chitosan nanoparticles and quercetin-loaded nanoparticles. Each value is expressed as mean $\pm$ SD ($n = 3$).

upon inclusion of fluorophores, chitosan nanoparticles offer a less polar and more rigid protective microenvironment shielding the excited species from the quenching and nonradiative decay processes, similar phenomenon had been observed by Zhu et al. who found that inclusion of fluorophoric reagents into β-cyclodextrins resulted in a range of fluorescent enhancement.[31]

Scavenging of DPPH radical

Free radicals are generated by normal metabolic process or from exogenous factors and agents, and they can easily initiate the peroxidation of membrane lipids, leading to the accumulation of lipid peroxides.[32] DPPH has a hydrogen free radical and shows a characteristic absorption at 517 nm.[33,34] While encountering the proton-radical scavengers, the purple color of the DPPH solution fades rapidly.[35] In the present study, DPPH was used to determine the proton-scavenging activity of the chitosan nanoparticles and quercetin-loaded nanoparticles.

Total DPPH scavenging potential of chitosan nanoparticles and quercetin-loaded nanoparticles at varying concentrations was measured and the results were depicted in Figure 8. In the DPPH test, quercetin-loaded nanoparticles were able to reduce the stable radical DPPH to the yellow colored diphenylpicrylhydrazine and the scavenging ability relied on the concentration of nanoparticles. It can be therefore concluded that the complexes formed maintained the quercetin antioxidant activity.

Reducing power of nanoparticles

It was reported there is a direct correlation between antioxidant activities and reducing power of some plant extracts.[36] Early research[37,38] found that the

reducing power are generally associated with the presence of reductones, which have been shown to exert antioxidant action by breaking the free radical chain through donating a hydrogen atom.

Figure 9. showed the reducing power of chitosan nanoparticles and quercetin-loaded nanoparticles. The reducing power of quercetin-loaded nanoparticles correlated well with increasing concentration. The results indicated that quercetin was effectively encapsulated in the chitosan nanoparticles and the reducing power of the inclusion complex was pronounced.

CONCLUSIONS

Chitosan nanoparticles and quercetin-loaded nanoparticles were prepared based on the ionic gelation of chitosan with TPP anions. Different analytical techniques, including AFM, DSC, XRPD, FTIR, UV-Vis, and fluorescence spectrum were adopted to characterize the inclusion compounds. These results showed that quercetin existing in an amorphous state was encapsulated in chitosan nanoparticles. The antioxidant activity of the quercetin-nanoparticles was also evaluated *in vitro* by two different methods, which indicated that encapsulation of quercetin in chitosan nanopaticles may be useful in improving the bioavailabilty of quercetin in pharmaceutical formulation.

References

1. Calabro, M. L.; Tommasini, S.; Donato, P.; Raneri, D.; Stancanelli, R.; Ficarra, P.; Ficarra, R.; Costa, C.; Catania, S.; Rustichelli, C.; Gamberini, G. J Pharm Biomed Anal 2004, 35, 365.
2. Walle, T. Free Radic Biol Med 2004, 36, 829.
3. Kaldas, M. I.; Walle, U. K.; van der Woude, H.; McMillan, J. M.; Walle, T. J Agric Food Chem 2005, 53, 4194.
4. Zheng, Y.; Haworth, I. S.; Zuo, Z.; Chow, M. S. S.; Chow, A. H. L. J Pharm Sci 2005, 94, 1079.
5. Formica, J. V.; Regelson, W. Food Chem Toxicol 1995, 33, 1061.
6. Schaab, M. R.; Barney, B. M.; Francisco, W. A. Biochemistry 2006, 45, 1009.
7. Pralhad, T.; Rajendrakumar, K. J Pharm Biomed Anal 2004, 34, 333.
8. Makris, D. P.; Rossiter, J. T. Quercetin and Rutin (quercetin 3-O-rhamnosylglucoside) Thermal Degradation in Aqueous Media Under Alkaline Conditions; Royal Society of Chemistry: Cambridge, 2000.
9. Gref, R.; Minamitake, Y.; Peracchia, M. T.; Trubetskoy, V.; Torchilin, V.; Langer, R. Science 1994, 263, 1600.
10. Wu, Y.; Yang, W.; Wang, C.; Hu, J.; Fu, S. Int J Pharm 2005, 295, 235.
11. Agnihotri, S. A.; Mallikarjuna, N. N.; Aminabhavi, T. M. J Control Release 2004, 100, 5.
12. Kumar, M. N. React Funct Polym 2000, 46, 1.

13. Kumar, M. N.; Muzzarelli, R. A.; Muzzarelli, C.; Sashiwa, H.; Domb, A. J. Chem Rev 2004, 104, 6017.
14. Illum, L.; Jabbal-Gill, I.; Hinchcliffe, M.; Fisher, A. N.; Davis, S. S. Adv Drug Deliv Rev 2001, 51, 81.
15. Sinha, V. R.; Singla, A. K.; Wadhawan, S.; Kaushik, R.; Kumria, R.; Bansal, K.; Dhawan, S. Int J Pharm 2004, 274, 1.
16. Sawayanagi, Y.; Nambu, N.; Nagai, T. Chem Pharm Bull 1983, 31, 2507.
17. Wittaya-areekul, S.; Kruenate, J.; Prahsarn, C. Int J Pharm 2006, 312, 113.
18. Illum, L.; Farraj, N. F.; Davis, S. S. Pharm Res 1994, 11, 1186.
19. Takeuchi, H.; Yamamoto, H.; Kawashima, Y. Adv Drug Deliv Rev 2001, 47, 39.
20. Mitra, S.; Gaur, U.; Ghosh, P. C.; Maitra, A. N. J Control Release 2001, 74, 317.
21. Vila, A.; Sanchez, A.; Tobio, M.; Calvo, P.; Alonso, M. J. J Control Release 2002, 78, 15.
22. Berger, J.; Reist, M.; Mayer, J. M.; Felt, O.; Peppas, N. A.; Gurny, R. Eur J Pharm Biopharm 2004, 57, 19.
23. Kawashima, Y.; Handa, T.; Kasai, A.; Takenaka, H.; Lin, S. Y.; Ando, Y. J Pharm Sci 1985, 74, 264.
24. Hari, P. R.; Chandy, T.; Sharma, C. P. J Appl Polym Sci 1996, 59, 1795.
25. Calvo, P.; Remunan-Lopez, C.; Vila-Jato, J. L.; Alonso, M. J. J Appl Polym Sci 1997, 63, 125.
26. Qi, L.; Xu, Z.; Jiang, X.; Hu, C.; Zou, X. Carbohydr Res 2004, 339, 2693.
27. Shimada, K.; Fujikawa, K.; Yahara, K.; Nakamura, T. J Agric Food Chem 1992, 40, 945.
28. Yen, G. C.; Chen, H. Y. J Agric Food Chem 1995, 43, 27.
29. Huang, H. Z.; Yang, X. R. Colloid Surface A 2003, 226, 77.
30. Sengupta, B.; Sengupta, P. K. Biochem Biophys Res Commun 2002, 299, 400.
31. Zhu, L. Z.; Qi, Z. H.; Lu, Z. S.; Jing, H.; Qi, W. B. Microchem J 1996, 53, 361.
32. Halliwell, B.; Gutteridge, J. M. C. Methods Enzymol 1990, 186, 1.
33. Di Mambro, V. M.; Azzolini, A. E.; Valim, Y. M.; Fonseca, M. J. Int J Pharm 2003, 262, 93.
34. Lin, H. Y.; Chou, C. C. Food Res Int 2004, 37, 883.
35. Yamaguchi, T.; Takamura, H.; Matoba, T.; Terao, J. Biosci Biotechnol Biochem 1998, 62, 1201.
36. Duh, P. D.; Du, P. C.; Yen, G. C. Food Chem Toxicol 1999, 37, 1055.
37. Ioku, K.; Tsushida, T.; Takei, Y.; Nakatani, N.; Terao, J. Biochim Biophys Acta 1995, 1234, 99.
38. Xing, R.; Yu, H.; Liu, S.; Zhang, W.; Zhang, Q.; Li, Z.; Li, P. Bioorg Med Chem 2005, 13, 1387.